

Co-manipulation of soft-materials estimating deformation from depth images

Giorgio Nicola^{1*}, Enrico Villagrossi¹ and Nicola Pedrocchi¹

¹Institute of Intelligent Industrial Technologies and Systems for Advanced Manufacturing, National Research Council of Italy, Via A. Corti 12, Milan, 20133, Italy.

*Corresponding author(s). E-mail(s): giorgio.nicola@stiima.cnr.it;

Abstract

Human-robot co-manipulation of soft materials, such as fabrics, composites, and sheets of paper/cardboard, is a challenging operation that presents several relevant industrial applications. Estimating the deformation state of the co-manipulated material is one of the main challenges. Viable methods provide the indirect measure by calculating the human-robot relative distance. In this paper, we develop a data-driven model to estimate the deformation state of the material from a depth image through a Convolutional Neural Network (CNN). First, we define the deformation state of the material as the relative roto-translation from the current robot pose and a human grasping position. The model estimates the current deformation state through a Convolutional Neural Network, specifically a DenseNet-121 pretrained on ImageNet. The delta between the current and the desired deformation state is fed to the robot controller that outputs twist commands. The paper describes the developed approach to acquire, preprocess the dataset and train the model. The model is compared with the current state-of-the-art method based on a skeletal tracker from cameras. Results show that our approach achieves better performances and avoids the various drawbacks caused by using a skeletal tracker. Finally, we also studied the model performance according to different architectures and dataset dimensions to minimize the time required for dataset acquisition.

Keywords: human-robot collaborative transportation, soft materials co-manipulation, vision-based robot manual guidance

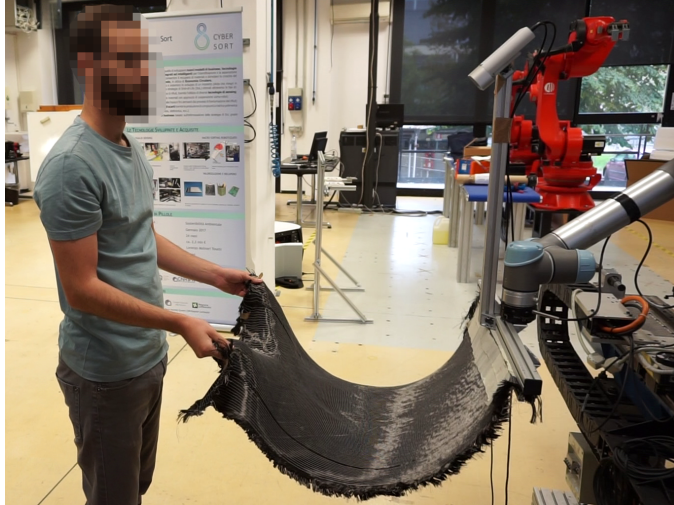


Fig. 1: The studied problem of human-robot collaborative transportation of a soft material. The human holds the co-manipulated object from one side and, through an RGB-D camera, estimates the object's deformation.

1 Introduction

Robots are increasingly assuming the role of assistants to humans in workplaces. However, robots still lack the intelligence to behave as helpful assistants. A paradigmatic application that highlights such limits is collaborative manipulation and transport, which is impactful in multiple fields of application, from industrial logistics and construction to households.

Human-Robot collaborative transportation offers multiple challenges. First, the robot might need to learn the path or the object's final position. The robot infers them based on clear signals from the human operator or via haptic communication through the co-manipulated object. However, in the co-manipulation of non-rigid objects, haptic communication is limited since not all forces and torques applied by the human can be read from the robot end-effector. Second, the robot should share the workload with the human. Still, the human should be able to gain control over the robot, i.e., the robot and human should be able to exchange leader and follower roles continuously [Franceschi, Pedrocchi, and Beschi \(2022\)](#). Finally, a well-known problem of manipulating large objects is the rotation-translation ambiguity in human-robot [Dumora, Geffard, Bidard, Brouillet, and Fraisse \(2012\)](#) co-manipulation, but it can arise even during human-human [Jensen, Salmon, and Killpack \(2021\)](#) co-manipulation.

In this paper, we study the problem of human-robot collaborative transportation of soft materials like fabric, shown in Figure 1. Unlike rigid objects, soft materials do not transfer compression forces since the absence of flexural

rigidity characterizes them. Furthermore, the rigidity along the other directions is also very low, and the amount of force/torques they can sustain without damage is minimal. Thus, estimating the deformation state only by force and torque measurements is challenging. Consequently, standard control architectures based on impedance or admittance control cannot be used directly [De Schepper, Moyaers, Schouterden, Kellens, and Demeester \(2021\)](#); [Sirintuna, Giammarino, and Ajoudani \(2022\)](#).

We propose to use a data-driven approach to develop a black-box model based on a Convolutional Neural Network (CNN), to estimate the deformation state of the co-manipulated soft material from depth images acquired by an RGB-D camera rigidly attached to the robot end-effector. Given a predefined rest configuration state, any estimated variation from such rest state caused by the human can be translated into a movement intention towards the direction that minimizes such difference. The proposed approach is applied to a case of human-robot collaborative transportation of a piece of carbon fiber fabric, proving the method's effectiveness.

The paper is structured as follows: in Section Introduction, related works and paper contributions are presented; in Section Method, the human-robot collaborative transportation problem is formalized, and the proposed solution, including the dataset acquisition strategy, is detailed; In Section Experiments, experimental evaluation of the approach is presented including comparison with state of the art, analysis of different neural network architectures and the dataset dimension; In section Conclusion, conclusions and future works are highlighted.

1.1 Related Work

The manipulation of deformable objects has been deeply investigated [Sanchez, Corrales, Bouzgarrou, and Mezouar \(2018\)](#), and multiple strategies have been developed, sometimes depending also on the geometric characteristics of the objects. Specifically, two main classes of deformable objects are studied: cables [She et al. \(2020\)](#); [W. Wang and Balkcom \(2018\)](#) and cloth-like [Mcconachie, Dobson, Ruan, and Berenson \(2020\)](#); [Miller et al. \(2012\)](#); [Verleysen, Biondina, and Wyffels \(2020\)](#). Manipulation of cloth-like objects is typically focused on the cloth folding task. However, few works study the problem of the collaborative human-robot manipulation of such objects; instead, they typically focus on cloth folding [Lee, Lu, Gupta, Levine, and Abbeel \(2015\)](#); [Li, Yue, Xu, Grinspun, and Allen \(2015\)](#). One of the main difficulties in manipulating deformable materials is tracking the object and estimating its current shape, that is, its deformation [Tang and Tomizuka \(2022\)](#). Two main approaches have been developed to estimate the material deformation in human-robot manipulation of deformable materials: human motion capture and direct deformation estimation of the material. In the first case, the deformation is estimated by tracking the position of the material grasped points by the robot and human by implementing a motion capture system based on either IMU sensors [Sirintuna et al. \(2022\)](#) or camera [Andronas, Kampourakis,](#)

et al. (2021). Tracking the grasping point in the space assumes that the position grasping point on the manipulated object is known as *a priori* or is detectable. Therefore, it is possible to completely reconstruct the shape of the manipulated material thanks to physics simulation software [Andronas, Kampourakis, et al. \(2021\)](#); [Kruse, Radke, and Wen \(2017\)](#) or directly use the human-robot relative distance as input to the controller [Sirintuna et al. \(2022\)](#). In the second case, the deformation is estimated using a camera to detect visual features on the manipulated material converted into robot commands. Different types of visual features have been developed in the literature. In [Kruse, Radke, and Wen \(2015\)](#), material folds are detected and combined with force measurements to compute robot speed commands directly. In [Jia, Hu, Pan, and Manocha \(2018\)](#); [Jia, Pan, Hu, Pan, and Manocha \(2019\)](#), Histograms of Oriented Wrinkles (HOWs) are implemented as visual features to detect deformations. HOWs are computed by applying Gabor filters and extracting the high-frequency and low-frequency components on the RGB image. Subsequently, in [Jia et al. \(2018\)](#), a controller converts the desired speed in the feature to the robot end effector speed. Meanwhile, in [Jia et al. \(2019\)](#), a Random Forest controller is trained to compute the desired robot grasping point position from the HOW feature space.

Finally, in [De Schepper et al. \(2021\)](#), a different approach is used. Instead of estimating the material deformation, motion tracking is used to detect hand-crafted coded gestures that, combined with torque force measures, are used directly to compute robot end effector speed.

Recently, Deep Neural Networks have been used as feature extractors via autoencoder networks [Tanaka, Arnold, and Yamazaki \(2018\)](#); [Tsurumine and Matsubara \(2022\)](#); [Yang et al. \(2017\)](#). The extracted feature is subsequently used to plan robot movement to achieve the desired deformation. However, none of those methods based on DNN feature extraction has been currently applied to human-robot manipulation.

The EU H2020 projects DrapeBot [DrapeBot Consortium \(2021\)](#) and Merging [MERGING Consortium \(2019\)](#) are pioneering actions coping with these challenges in the industrial scenario. The DrapeBot project focuses on the robotic manipulation of carbon fiber and fiberglass plies during the draping process; in particular, [Eitzinger, Frommel, Ghidoni, and Villagrossi \(2021\)](#) highlights the importance of the human-robot co-manipulation when the dimension of the ply is such as to require more than one robot. The project Merging looks at the manipulation of flexible and fragile objects exploiting multiple industrial robots, designing new Electro-Adhesive (EA) grasping devices, using information from perception systems fused with the data from a digital twin to estimate the deformations of flexible elements [Andronas, Kokotinis, and Makris \(2021\)](#); [Makris, Kampourakis, and Andronas \(2022\)](#).

1.2 Contribution

This paper proposes to combine the two main approaches in the literature to estimate the material deformation by calculating the relative distance between



Fig. 2: Example of two different human grasping configurations on a carbon fiber ply. As can be noticed in both grasping configurations, the human hands do not introduce any deformation on the material between them. Thus, the portion of material between them can be considered rigid, and a single arbitrary point on the human side of the ply is sufficient to describe its position

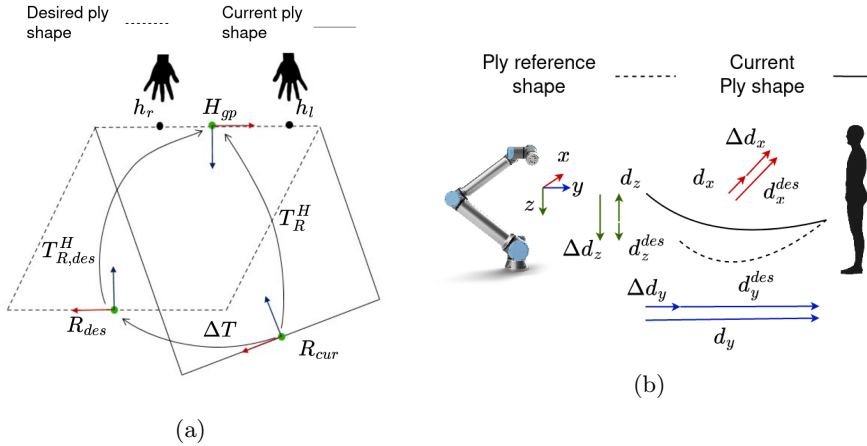


Fig. 3: Proposed formalization of the human-robot collaborative transportation problem. a) Shows the top view highlighting the definition of the human grasping point H_{gp} . b) Shows a lateral view highlighting the parameters that compose T_R^H , $T_{R,des}^H$, and ΔT . For the sake of simplicity, rotations have been neglected.

the robot and human grasping position directly from the material rather than from a motion tracking system. The human-robot relative pose is estimated through a convolutional deep neural network fed with the depth image of the handled material. The robot controller is designed to minimize the distance between the estimated relative pose and a rest relative pose.

Using depth images has multiple advantages compared to state-of-the-art solutions. First, motion tracking-based methods assume to know exactly how

the human will grasp the object because either defined *a priori* or detected. However, such an assumption is only sometimes realistic, especially in unstructured environments such as factories and households. Our method does not track the hands, but it estimates the robot pose w.r.t. the human hands by looking at the deformation of the material.

Second, motion tracking-based methods strongly rely on the sensor's performance. On the one hand, IMU-based motion tracking is affected by a drift that can only be corrected with other motion capture techniques based on cameras or re-calibrating the setup. IMU, in addition, must be worn by the operator either with straps or specific suits that are uncomfortable for the operator, they can slide, and their position on the body is not repeatable. On the other hand, camera-based motion capture has the disadvantage that it has a limited working range both in the distance and in the field of view, and it is sensible for occlusions unless multiple cameras are used.

Third, the proposed approach does not rely on handcrafted features as usually the methods that look at the material estimation do. On the one hand, the features might only partially describe the studied problem. On the other hand, transforming the feature space into robot commands takes a lot of work. Indeed, specific controllers are used, and in some cases, imitation learning on expert user samples is adopted.

Finally, our methodology avoids any use of force/torque feedback. Such sensors are very noisy, limited bandwidth, and have high oscillations due to the object-handled dynamics. Furthermore, we avoid translation/rotation ambiguity.

2 Method

2.1 Problem formulation

The problem of human-robot collaborative manipulation of soft materials is composed of two agents handling the soft material simultaneously, as shown in Figure 1. One agent is the human that leads the activity, and the second one is the robot that should follow the human movement. The objective is to manipulate the desired object while minimizing the deformations from a rest configuration that guarantees no damage to the material.

Soft materials, like fabric, can be approximated as membranes [Vasiliev and Morozov \(2018\)](#) characterized by the absence of flexural rigidity. Therefore, they cannot sustain compressive loads, and deformations can be caused only by displacements or traction forces.

Let us consider a soft material from now on called ply handled by two agents, a human and a robot. Denote h_r and h_l as the human's hands grasping positions, and R_{cur} as the robot's current grasping point. Given the assumption that the gripper geometry is constant, it is easy to see that a bi-unique proxy for the ply shape is the tuple of the relative roto-translations between the robot grasping position and the human hands holding positions, except for the local deformation around the hands that may change from person to

person. This model, however, is unnecessarily accurate since it also models the deformation of the ply in the corners, i.e., the roto-translation might change not only according to the distance human-robot but also to where the humans are grasping.

A further likely assumption is that the human tenses the fabric between the hands, achieving a minimal internal tension of the ply, not enough to deform it but compensating for the gravity deformation effect. The material between the two hand-grasping points can be considered rigid in such a condition. Given this assumption, it is possible to define an arbitrary point on the ply between the hands invariant to the different grasping positions, Figure 2. The relative roto-translations between the robot grasping position and this point is a robust proxy for the ply deformation, except for the local deformation around the hands and the geometry of the corners, which are irrelevant to the control objective.

Mathematically, denote H_{gp} as the proxy for the single human grasping point (Figure 3a). Denoting T_R^H and $T_{R,des}^H$ as the actual roto-translation matrix between R_{cur} and H_{gp} and a target desired ply shape. Given this formulation, the problem consists of (i) imposing the target $T_{R,des}^H$ and (ii) estimating T_R^H during the execution movement. The robot should be controlled based on such estimations to minimize the distance from the target's desired pose.

As a final note, given the frame reference in Figure 3b, a further simplifying assumption is that the x -axis rotation is always zero since it does not cause macroscopic deformations of the ply but only local deformations.

2.2 Proposed solution

We estimate the roto-translation T_R^H through an ensemble of CNNs that takes as input a depth image of the material from a camera rigidly attached to the robot end-effector. Specifically, the ensemble of CNNs outputs the parameters that fully describe T_R^H , i.e., three translations and two rotations following the xyz Euler conventions. For this purpose, an RGB-D camera is rigidly attached to the robot end-effector that looks at the top of the co-manipulated element, allowing the easy detection of the material shape and deflections due to the forces/displacement applied by the human on the material (see Figure 1). The 3D camera provides the depth map, and after proper preprocessing, a depth map is obtained composed only of carbon fiber ply segmented from the background and the human partner. The segmented depth map is fed to an ensemble of CNNs trained to estimate the deformation of the material, in other words, the distance between the robot gripper and the human grasping point H_{gp} . Applying Deep Learning techniques allows for defining a black-box model describing the relation between visual deformation and mechanical status.

2.3 Dataset acquisition

The training of the dataset should be done by acquiring a large number of depth images of the deformed material with different human-robot relative

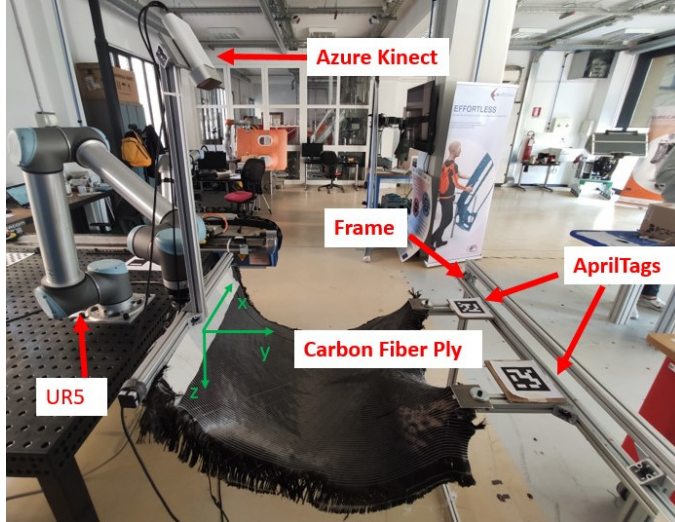


Fig. 4: The setup developed to acquire the dataset of a carbon fiber ply. The setup comprises an RGB-D camera, Azure Kinect, a robot Universal Robot UR5, an aluminum frame to mimic the human, and a pair of fiducial markers, Apriltags, to localize the frame.

distances and human grasping positions. To avoid a bothering effort to a human operator, we substituted the human with a frame that holds the soft material to achieve higher accuracy and repeatability of the dataset, as shown in Figure 4, and the relative distance is got by moving the robot and maintaining the frame fix.

Precisely, a pair of metallic clips mimic the effect of the hands holding the ply. The frame allows the simulation of different human grasping positions on the material from now on, called human grasping configurations (Figure 2). The frame's position is estimated using a pair of Apriltags [J. Wang and Olson \(2016\)](#), and the robot is moved relative to the frame. At each robot position, a set of RGB-D images are taken to account for the camera's noisy output.

The manipulated material is segmented from the background. First, the depth image is thresholded to a maximum and minimum value, and all pixels whose value is not within this range are set to zero to remove far and close objects quickly. Second, to remove the frame, Apriltags are used, the RGB image is converted into grayscale, and the tags' positions in the 2D picture are detected. Subsequently, a parallel line to the line passing by the tags is drawn, and all the pixels above this line are set to zero. Finally, each image is cropped and resized to the resolution of 224×224 . Each image is autonomously labeled with 3 Cartesian translations and the two rotations that fully describe T_R^H as in Section Problem formulation.

3 Experiments

3.1 Experimental setup

We tested the method with a piece of carbon fiber fabric with dimensions $90 \times 60 \text{ cm}$. Given a desired rest configuration of $x_{ref} = 0.0 \text{ m}$, $y_{ref} = 0.6 \text{ m}$, $z_{ref} = 0.0 \text{ m}$, $\theta_{ref} = 0.0^\circ$, $\gamma_{ref} = 0.0^\circ$ the dataset of the deformed material was acquired in the range of $\pm 0.105 \text{ m}$ with step 0.03 m on the $x - y - z$ axes and $\pm 20^\circ$ with step 5° on both y and z axis rotations for a total of 41472 different poses for each human grasping configuration of the material. The dataset resolution is the maximum permissible estimation error of the roto-translation matrix parameters. Furthermore, the study considered 9 different human grasping configurations and 746496 depth images, *i.e.*, two depth images were taken for each robot position. The setup for acquiring the dataset included an RGB-D camera, an Azure Kinect, and a Universal Robot UR5 as a robotic platform.

3.2 Human Robot co-manipulation evaluation

3 CNN models with Densenet-121 [Huang, Liu, Van Der Maaten, and Weinberger \(2017\)](#) compose of the system. The optimization software Optuna [Akiba, Sano, Yanase, Ohta, and Koyama \(2019\)](#) has computed the hyperparameters. The three input channels of the first convolutional layer of the Densenet-121 were substituted with a convolutional layer with one input channel. This design choice is because the proposed method uses only depth images, while Densenet-121 is pretrained on the ImageNet dataset [Deng et al. \(2009\)](#) composed of RGB images. The weights of the new layer are equal to the sum of the weights along the three original channels. Figure 5 shows the error distributions of the estimation of the various parameters of T_R^H as boxplots.

Subsequently, we compared our approach against the commonly used method in literature based on tracking the hands' positions with a camera-based skeletal tracker and computing the human-robot distance. Therefore, the same Azure Kinect is used to acquire depth images of the human and perform skeletal tracking. The methods comparison exploited the same setup used for the dataset acquisition, the only difference being that a human was pretending to grasp the deformable material. The depth image segmentation does not use the Apriltags to simulate actual operating conditions for the model. In contrast, it uses the hands' key points positions in the 2D depth image, computed with the skeletal tracker from Azure Kinect. It is essential to note that the skeletal tracker is used for segmenting the depth image only for convenience since developing a method for segmenting the ply is out of the scope of this work. Any method to segment the co-manipulated material can be implemented based or not on a skeletal tracker. Finally, the robot was positioned in 20 known relative poses to the frame, *i.e.*, set the material with a known deformation state, and we compared both methods on 20 frames for each pose. Results are shown in Figure 6.

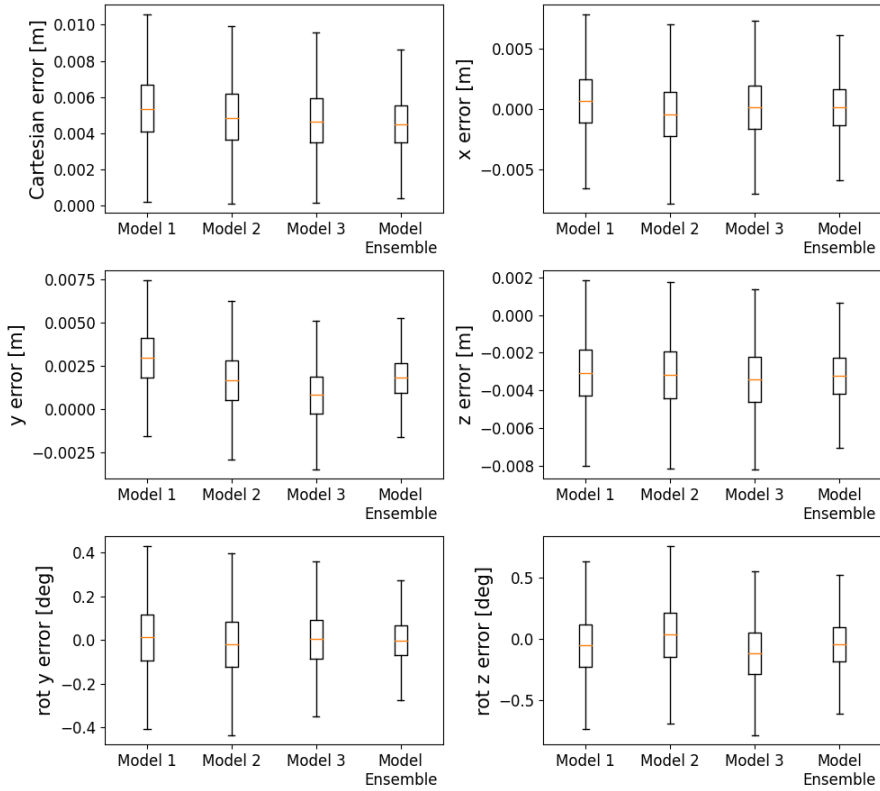


Fig. 5: Comparison between the results of the single models and the model ensemble. **Top left** Cartesian estimation error. **Top right** estimation error on the x -axis. **Center left** estimation error on the y -axis. **Center right** estimation error on the z -axis. **Bottom left** estimation error on the y -axis rotation. **Bottom right** estimation error on the z -axis rotation.

First, the CNN model estimation error on the x and z axis is sensibly lower and similar on y . The estimation error on the rotations is slightly higher but similar to the skeletal tracking error.

Second, the error of the CNN model compared to the test dataset's error (Figure 5) is significantly higher. The authors believe that this difference depends on the various sources of inaccuracies in the experimental setup rather than overfitting on the ply segmentation. Indeed, the robot grasping position and the frame grasping position are hard to reproduce.

The same preprocessing pipeline of the dataset acquisition leads to similar results for the model. Even a tiny error in the grasping position, less than 1 cm, can significantly change the material shape when highly stretched. Indeed, note that the error in the deformation estimation is concentrated in those poses

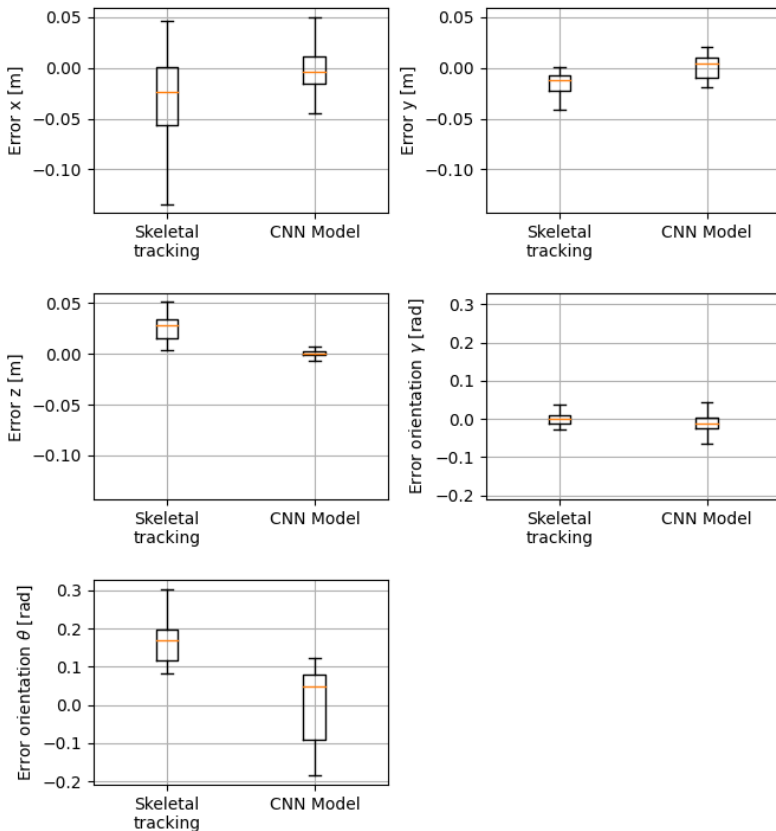


Fig. 6: Comparison of the error distributions in estimating the deformation state between the method used in literature based on skeletal tracking and our method based on a CNN model. **Top left** estimation error on the x-axis. **Top right** estimation error on the y-axis. **Center left** estimation error on the z-axis. **Center right** estimation error on y-axis rotation. **Bottom left** estimation error on the z-axis rotation.

with high values of θ and γ rotations; nevertheless, the rotation was usually underestimated when the ply was highly stretched.

In conclusion, the proposed approach proved to have a better estimation in the x , y , and z positions while slightly worse in the rotation. However, the skeleton tracker method was tested only in optimal conditions, i.e., when the distance camera key points are below 2.5 m when using the broad field of view. Indeed, as described in Tölgessy, Dekan, and Chovanec (2021), the skeletal tracking accuracy of the Azure Kinect drastically deteriorates above a threshold distance depending on the used field of view, thus, directly limiting the maximum size of the co-manipulated material.

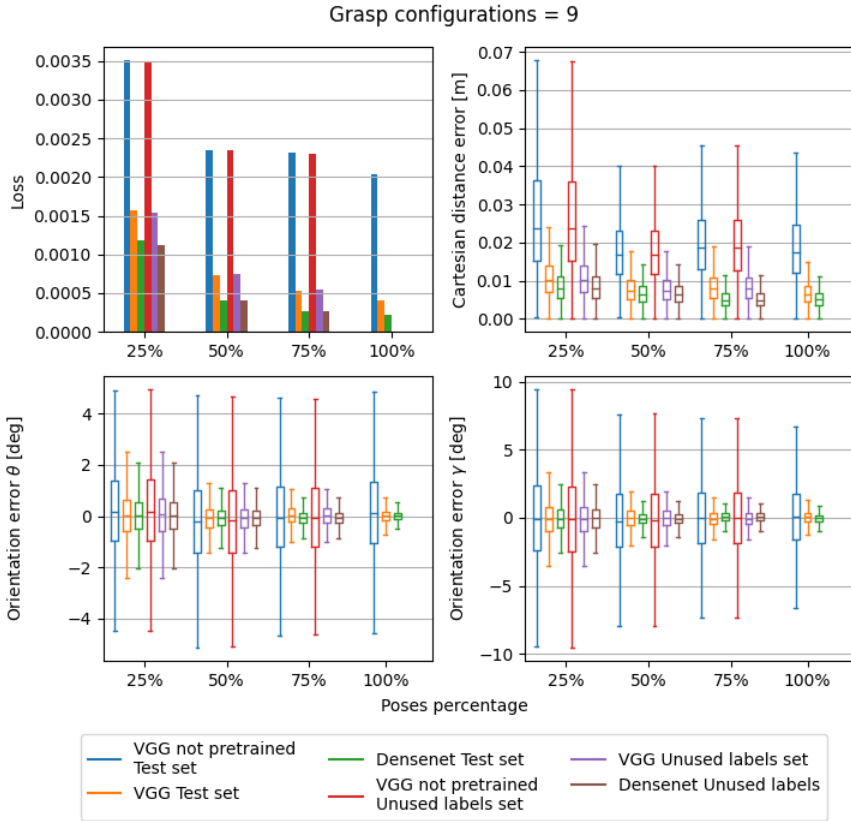


Fig. 7: Training results of VGG not pretrained, VGG pretrained, and Densenet121 on the different percentage of the dataset. **Top left** shows the average loss for each architecture on the test dataset and the unused dataset. **Top right** shows the Cartesian distance error for each architecture as a boxplot. **Bottom left** shows the orientation error on the y-axis for each architecture as a boxplot. **Bottom right** shows the orientation error on the z-axis for each model as a boxplot.

3.3 Network architecture analysis

In this section, we studied the model accuracy using different network architectures. The network architectures studied were the following: a VGG11 without initialized parameters as in [Nicola, Villagrossi, and Pedrocchi \(2022\)](#), VGG11 [Simonyan and Zisserman \(2015\)](#) with batch normalization provided by PyTorch and Densenet-121 [Huang et al. \(2017\)](#) provided by PyTorch [Paszke et al. \(2019\)](#).

The learning rate is equal once to 1×10^{-4} , and batch size is 256 on three different validation sets. The same conditions were applied to each combination of architecture and dataset dimension to evaluate them in the same situation.

After the first 5 epochs without improvements, the learning rate was divided by 10; otherwise, the training was stopped. The maximum number of epochs was 45.

Figure 7 shows the training results of each architecture on different percentages of the dataset, including loss and distributions of the Cartesian distance error and orientation error over the y and z axis. It is worth noting that VGG11 and Densenet121 achieve far better results on the test dataset than the VGG not pretrained. This result confirms our hypothesis that the feature learned on the ImageNet dataset are still beneficial even though the input image type is different. Furthermore, similarly to the results on ImageNet, DenseNet121 achieved better results than VGG11.

Subsequently, each architecture is trained on a different percentage of the dataset to verify whether a reduced-dimension dataset can still generalize on unseen data. In particular, results are compared between the test dataset and the unused dataset (set of labels removed from the dataset before dividing between training and test dataset). Not surprisingly, for every network architecture, the model performances decrease with the dataset size, with a significant drop at 25%. However, the loss values and the error distributions are almost identical between the test set and the unused set. It is possible to deduce that 1/4 of the acquired dataset with the deformation range is enough to train a model to generalize over unseen data and specifically unseen deformation combinations. Indeed, in Densenet121 on 25% of the data points in both the test and the unused datasets, the error is far below the dataset resolution (0.03 m on the x - y - z axis and 5° on θ and γ rotations). Increasing the dataset size, however, is still beneficial to improve the model's accuracy.

3.4 Dataset dimension analysis

The dataset dimension plays an essential role in the training time, which is still a relevant obstacle to implementing Deep Learning methods in the industry.

Three main factors influence the dataset dimension for the presented use case: (i) the number of photos for each pose; (ii) the number of poses for each human grasping configuration; (iii) the number of human grasping configurations.

However, the first point's relevance is minimal since most of the time during the dataset acquisition is spent moving the robot from one pose to another. The photo acquisition takes 0.03s while the time point-to-point motion takes 0.2 s.

The design of the experiments for study for the dataset dimension analysis foresees investigations with [100%, 75%, 50%, 25%] over the 373.248 poses randomly chosen before mentioned and [6, 4] human grasping configurations. Only Densenet121 was studied since it achieved the best performances in all previous training conditions. Each experiment provides the same training conditions of the network architecture analysis.

We compared the results among the test dataset, the “unused labels set”, and the “unused grasp set”. Specifically, the ‘unused label set’ includes all

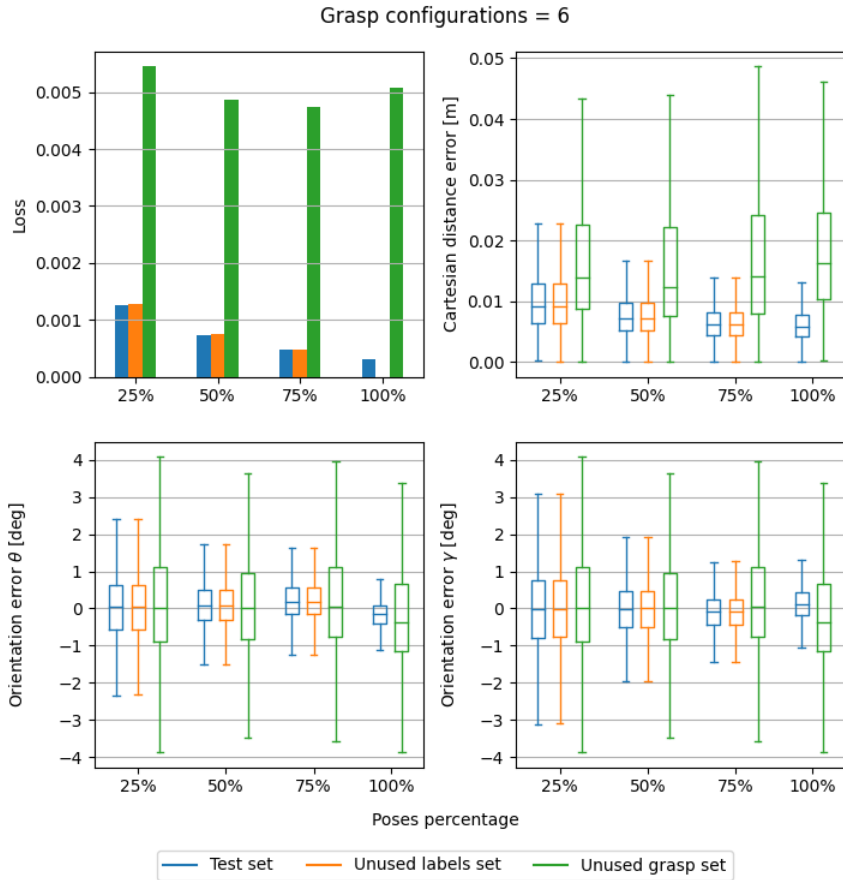


Fig. 8: Results training of the DenseNet121 on the different percentages of the dataset and including only six grasp configurations over 9. **Top left** shows the loss for each model on the test dataset and the unused dataset. **Top right** shows the Cartesian distance error for each model as a boxplot. **Bottom left** shows the orientation error on the y-axis for each model as a boxplot. **Bottom right** shows the orientation error on the z-axis for each model as a boxplot.

the datapoints in the unused set with the grasp configurations on which it is trained. The “unused grasp set” groups all the datapoints in the unused set with a discarded grasp configuration.

Figure 8 and Figure 9 reports the models result with 6, and 4 grasp configurations. Similarly to the case with all nine grasp configurations, results between the test set and the unused label set are almost identical. On the contrary, there is a significant difference in the results on the unused grasp set. Such results prove that generalizing over unseen grasping configurations is much more challenging than generalizing over unseen poses. Thus, the dataset

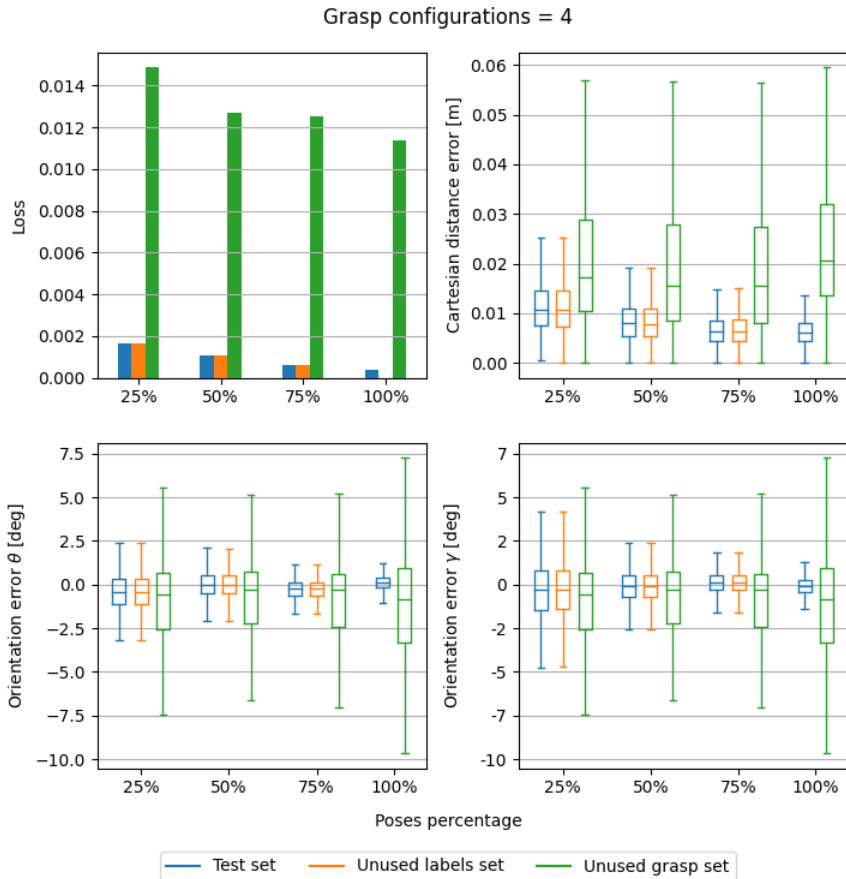


Fig. 9: Results training of the DenseNet121 on the different percentage of the dataset and including only four grasp configurations over 9. **Top left** shows the loss for each model on the test dataset and the unused dataset. **Top right** shows the Cartesian distance error for each model as a boxplot. **Bottom left** shows the orientation error on the y-axis for each model as a boxplot. **Bottom right** shows the orientation error on the z-axis for each model as a boxplot.

acquisition should focus on acquiring data with many grasping configurations rather than all the poses. Nevertheless, note that the worst performing model, trained on only 4 grasp configurations and 25% of training poses, estimates the Cartesian position with an error below the dataset resolution in more than 75% of the datapoints.

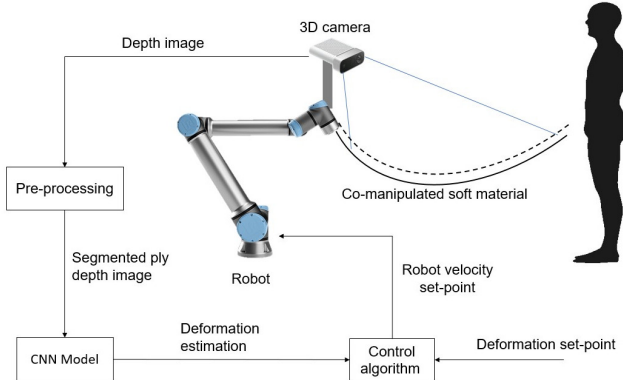


Fig. 10: Description of the developed pipeline to perform human-robot collaborative transportation.

3.5 Human-robot collaborative transportation

Refer to a scenario of human-robot collaborative transportation of carbon fiber fabric, as shown in Figure 1. The developed model is used to estimate the current deformation state of the carbon fiber fabric, and the difference concerning a predefined rest deformation state is converted into a twist command through a proportional controller as shown in Figure 10. A single PC runs the model and the robot controller, with a CPU, Intel Core i7-8700, and a GPU, NVIDIA GeForce RTX 3080Ti. The preprocessing run at approximately 30 Hz, and the robot controller with the model runs at 20 Hz. The user could smoothly move the co-manipulated material avoiding excessive material deformations as shown in the video in [Nicola \(2022\)](#).

4 Conclusions

This work presented a data-driven approach to co-manipulating soft deformable materials based on estimating the material deformation from depth images from an RGB-D camera rigidly attached to the robot end-effector through a CNN model. First, we formalized the problem of human-robot co-manipulation, and we defined the material deformation state based on the roto-translation between the robot grasping point and the human grasping point. Second, we developed a Deep Learning model to estimate the roto-translation matrix parameters from a depth image of the deformed material.

The proposed approach was compared with a well-known method from literature based on computing the human-robot distance as the distance between the robot and the human hand keypoints obtained via a camera-based skeleton tracker. Our approach proved more accurate and is not affected by the two main drawbacks of skeletal trackers. First, the human must always be in the camera's field of view, and second, the accuracy of the skeletal tracker tends

to decrease as the human-camera distance increases. Those two drawbacks can have an extremely negative effect when the co-manipulated material is significant. Meanwhile, our approach can estimate the deformation state of material with any dimension since it only looks at the co-manipulated material.

We evaluated multiple network architectures from the literature and studied the model performances according to dataset dimension. Indeed, one of the main limitations to applying Deep Learning models in the industry is the necessity of acquiring large datasets, which is time-consuming. Results showed that the dataset could be acquired with a much lower resolution than the desired maximum estimation error. On the other hand, results also showed that the number of grasping configurations in the dataset is critical since reducing them causes a significant drop in model performances.

Finally, the approach was tested in a real-world application of human-robot collaborative transportation of a carbon fiber fabric. The robot was able to follow human movements smoothly, avoiding excessive deformations.

The main drawback of the proposed approach is that it needs quite a large dataset for every co-manipulated object that, even if it can be acquired chiefly autonomously, is still time-consuming. In future works, the authors will investigate the usage of synthetic datasets to train the model. Furthermore, we will train multiple models simultaneously, one for each ply shape, sharing a standard backbone for the CNN part of the network. Thus, the models should learn standard and possibly more general features that allow transfer learning by retraining the last fully connected layers. Finally, the deformation estimation was applied to the case of collaborative transportation with an anthropomorphic manipulator. The authors plan to apply the proposed approach to a case with an anthropomorphic manipulator mounted on top of a mobile platform to increase the technological fallout of the method.

Acknowledgments. This project has received funding from the European Union’s Horizon 2020 research and innovation program under grant agreement No 101006732, ”DrapeBot – A European Project developing collaborative draping of carbon fiber parts.”

References

Akiba, T., Sano, S., Yanase, T., Ohta, T., Koyama, M. (2019). Optuna: A next-generation hyperparameter optimization framework. *Proceedings of the 25th ACM SIGKDD international conference on knowledge discovery & data mining* (p. 2623–2631). New York, NY, USA: Association for Computing Machinery. Retrieved from <https://doi.org/10.1145/3292500.3330701>

Andronas, D., Kampourakis, E., Bakopoulou, K., Gkournelos, C., Angelakis, P., Makris, S. (2021). Model-based robot control for human-robot flexible material co-manipulation. *2021 26th IEEE international conference on*

emerging technologies and factory automation (etfa) (p. 1-8). 10.1109/ETFA45728.2021.9613235

Andronas, D., Kokotinis, G., Makris, S. (2021). On modelling and handling of flexible materials: A review on digital twins and planning systems. *Procedia CIRP*, 97, 447-452. (8th CIRP Conference of Assembly Technology and Systems)

<https://doi.org/10.1016/j.procir.2020.08.005>

De Schepper, D., Moyaers, B., Schouterden, G., Kellens, K., Demeester, E. (2021). Towards robust human-robot mobile co-manipulation for tasks involving the handling of non-rigid materials using sensor-fused force-torque, and skeleton tracking data. *Procedia CIRP*, 97, 325-330. Retrieved from <https://www.sciencedirect.com/science/article/pii/S2212827120314670> (8th CIRP Conference of Assembly Technology and Systems)

<https://doi.org/10.1016/j.procir.2020.05.245>

Deng, J., Dong, W., Socher, R., Li, L.-J., Li, K., Fei-Fei, L. (2009). Imagenet: A large-scale hierarchical image database. *2009 ieee conference on computer vision and pattern recognition* (p. 248-255). 10.1109/CVPR.2009.5206848

DrapeBot Consortium (2021). *Drapebot – a european project developing collaborative draping of carbon fiber parts.* Retrieved from <https://www.drapebot.eu/>

Dumora, J., Geffard, F., Bidard, C., Brouillet, T., Fraisse, P. (2012). Experimental study on haptic communication of a human in a shared human-robot collaborative task. *2012 IEEE/RSJ International Conference on Intelligent Robots and Systems*, 5137-5144.

Eitzinger, C., Frommel, C., Ghidoni, S., Villagrossi, E. (2021). System concept for human-robot collaborative draping. *Sampe europe conference* (p. 7542-7549).

Franceschi, P., Pedrocchi, N., Beschi, M. (2022). Adaptive impedance controller for human-robot arbitration based on cooperative differential game theory. *2022 international conference on robotics and automation (icra)* (p. 7881-7887). 10.1109/ICRA46639.2022.9811853

Huang, G., Liu, Z., Van Der Maaten, L., Weinberger, K.Q. (2017). Densely connected convolutional networks. *2017 ieee conference on computer vision and pattern recognition (cvpr)* (p. 2261-2269). 10.1109/CVPR

.2017.243

Jensen, S.W., Salmon, J.L., Killpack, M.D. (2021). Trends in haptic communication of human-human dyads: Toward natural human-robot co-manipulation. *Frontiers in Neurorobotics*, 15. Retrieved from <https://www.frontiersin.org/articles/10.3389/fnbot.2021.626074>

10.3389/fnbot.2021.626074

Jia, B., Hu, Z., Pan, J., Manocha, D. (2018). Manipulating highly deformable materials using a visual feedback dictionary. *2018 ieee international conference on robotics and automation (icra)* (p. 239-246). 10.1109/ICRA.2018.8461264

Jia, B., Pan, Z., Hu, Z., Pan, J., Manocha, D. (2019). Cloth manipulation using random-forest-based imitation learning. *IEEE Robotics and Automation Letters*, 4(2), 2086-2093.

10.1109/LRA.2019.2897370

Kruse, D., Radke, R.J., Wen, J.T. (2015). Collaborative human-robot manipulation of highly deformable materials. *2015 ieee international conference on robotics and automation (icra)* (p. 3782-3787). 10.1109/ICRA.2015.7139725

Kruse, D., Radke, R.J., Wen, J.T. (2017). Human-robot collaborative handling of highly deformable materials. *2017 american control conference (acc)* (p. 1511-1516). 10.23919/ACC.2017.7963167

Lee, A.X., Lu, H., Gupta, A., Levine, S., Abbeel, P. (2015). Learning force-based manipulation of deformable objects from multiple demonstrations. *2015 ieee international conference on robotics and automation (icra)* (p. 177-184). 10.1109/ICRA.2015.7138997

Li, Y., Yue, Y., Xu, D., Grinspun, E., Allen, P.K. (2015). Folding deformable objects using predictive simulation and trajectory optimization. *2015 ieee/rsj international conference on intelligent robots and systems (iros)* (p. 6000-6006). 10.1109/IROS.2015.7354231

Makris, S., Kampourakis, E., Andronas, D. (2022). On deformable object handling: Model-based motion planning for human-robot co-manipulation. *CIRP Annals*, 71(1), 29-32. Retrieved from <https://www.sciencedirect.com/science/article/pii/S0007850622000956>

<https://doi.org/10.1016/j.cirp.2022.04.048>

Mcconachie, D., Dobson, A., Ruan, M., Berenson, D. (2020). Manipulating deformable objects by interleaving prediction, planning, and control. *The International Journal of Robotics Research*, 39, 957 - 982.

MERGING Consortium (2019). *Manipulation enhancement through robotic guidance and intelligent novel grippers (merging)*. Retrieved from <http://www.merging-project.eu/>

Miller, S., van den Berg, J.P., Fritz, M., Darrell, T., Goldberg, K., Abbeel, P. (2012). A geometric approach to robotic laundry folding. *The International Journal of Robotics Research*, 31, 249 - 267.

Nicola, G. (2022). *Co-manipulation of soft-materials estimating deformation from depth images*. <https://doi.org/10.5281/zenodo.7300247>. ([Online; accessed 10-November-2022])

Nicola, G., Villagrossi, E., Pedrocchi, N. (2022). Human-robot co-manipulation of soft materials: enable a robot manual guidance using a depth map feedback. *2022 31st ieee international conference on robot and human interactive communication (ro-man)* (p. 498-504). 10.1109/RO-MAN53752.2022.9900710

Paszke, A., Gross, S., Massa, F., Lerer, A., Bradbury, J., Chanan, G., ... Chintala, S. (2019). Pytorch: An imperative style, high-performance deep learning library. *Advances in neural information processing systems 32* (pp. 8024-8035). Curran Associates, Inc. Retrieved from <https://proceedings.neurips.cc/paper/2019/file/bdbca288fee7f92f2bfa9f7012727740-Paper.pdf>

Sanchez, J., Corrales, J.-A., Bouzgarrou, B.-C., Mezouar, Y. (2018). Robotic manipulation and sensing of deformable objects in domestic and industrial applications: a survey. *The International Journal of Robotics Research*, 37(7), 688-716. Retrieved from <https://doi.org/10.1177/0278364918779698> <https://arxiv.org/abs/https://doi.org/10.1177/0278364918779698> 10.1177/0278364918779698

She, Y., Wang, S., Dong, S., Sunil, N., Rodriguez, A., Adelson, E.H. (2020). Cable manipulation with a tactile-reactive gripper. *The International Journal of Robotics Research*, 40, 1385 - 1401.

Simonyan, K., & Zisserman, A. (2015). Very deep convolutional networks for large-scale image recognition. *CoRR*, *abs/1409.1556*.

Sirintuna, D., Giammarino, A., Ajoudani, A. (2022). Human-robot collaborative carrying of objects with unknown deformation characteristics. *ArXiv*, *abs/2201.10392*.

Tanaka, D., Arnold, S., Yamazaki, K. (2018). Emd net: An encode-manipulate-decode network for cloth manipulation. *IEEE Robotics and Automation Letters*, *3*(3), 1771-1778.

10.1109/LRA.2018.2800122

Tang, T., & Tomizuka, M. (2022). Track deformable objects from point clouds with structure preserved registration. *The International Journal of Robotics Research*, *41*, 599 - 614.

Tölgessy, M., Dekan, M., Chovanec, L. (2021). Skeleton tracking accuracy and precision evaluation of kinect v1, kinect v2, and the azure kinect. *Applied Sciences*, *11*(12). Retrieved from <https://www.mdpi.com/2076-3417/11/12/5756>

10.3390/app11125756

Tsurumine, Y., & Matsubara, T. (2022). Variationally autoencoded dynamic policy programming for robotic cloth manipulation planning based on raw images. *2022 ieee/sice international symposium on system integration (sii)* (p. 416-421). 10.1109/SII52469.2022.9708850

Vasiliev, V.V., & Morozov, E.V. (2018). *Chapter 8 - equations of the applied theory of thin-walled composite structures* (Fourth Edition ed.). Elsevier. Retrieved from <https://www.sciencedirect.com/science/article/pii/B9780081022092000086> <https://doi.org/10.1016/B978-0-08-102209-2.00008-6>

Verleysen, A., Biondina, M., Wyffels, F. (2020). Video dataset of human demonstrations of folding clothing for robotic folding. *The International Journal of Robotics Research*, *39*, 1031 - 1036.

Wang, J., & Olson, E. (2016). Apriltag 2: Efficient and robust fiducial detection. *2016 ieee/rsj international conference on intelligent robots and systems (iros)* (p. 4193-4198). 10.1109/IROS.2016.7759617

Wang, W., & Balkcom, D.J. (2018). Knot grasping, folding, and re-grasping. *The International Journal of Robotics Research*, *37*, 378 - 399.

Yang, P.-C., Sasaki, K., Suzuki, K., Kase, K., Sugano, S., Ogata, T. (2017).

Repeatable folding task by humanoid robot worker using deep learning.

IEEE Robotics and Automation Letters, 2(2), 397-403.

10.1109/LRA.2016.2633383